Design of Complementary Filter for High-fidelity Attitude Estimation based on Sensor Dynamics Compensation with Decoupled Properties

Ken Masuya, Tomomichi Sugihara and Motoji Yamamoto

***Abstract*— A high-fidelity attitude estimation technique for wide and irregular movements is proposed, in which heterogeneous inertial sensors are combined in complementary way. Although the working frequency ranges of each sensor are not necessarily complementary, inverse sensor models are utilized in order to restore the original movements. In the case of 3D rotation, the sensor dynamics displays a highly nonlinear property. Even if it is approximated by a linear system, the inverse model of a sensor tends to be non-proper and unstable. An idea is to decouple it into the dynamics compensation part approximated by a linear transfer function and the strictly nonlinear coordinate transformation part. Bandpass filters inserted before the coordinate transformation guarantee that the total transfer function becomes proper and stable. Particularly, the differential operator of a high-pass filter cancels the integral operator included in the dynamics compensation of the rate gyroscope, which causes instability. The proposed method is more beneficial than Kalman filter in terms of the implementation since it facilitates a systematic design of the filter.**

I. Introduction

Attitude estimation is a crucial issue for the control of mobile machines such as aero crafts, unmanned vehicles and legged robots, especially when they move irregularly over wide spatial area. For this purpose, so-called inertial sensors including accelerometers, inclinometers and rate gyroscopes are used. However, each individual sensor has its own drawback. An inclinometer and an accelerometer, which find the direction of gravity in stationary state, are easily disturbed by dynamic translational movements. Since a rate gyroscope only measures the deviation of angular movement, integration of the output signal is required in order to estimate the absolute attitude, so that it often diverges due to the accumulation of drifts. For high-fidelity attitude estimation, it is necessary to combine those heterogeneous sensor outputs to complement inperfections of each other.

Kalman filter[1][2][3][4] is one of the frequently-used tool to pickup relevant information from mixed signals. A particular problem is that it is hard to tune the design parameters for reliable estimation, since how to characterize sensor signals in time domain is not trivial. On the other hand, complementary filter[5][6][7][8][9][10][11] is rather a promising technique, where it is designed in frequency domain. The frequency response analysis of each sensor tells its working frequency range. The problem is that those working ranges of each sensor are not necessarily complementary, so that the accuracy of estimation is possibly degraded against movements in particular frequency range. An idea to resolve these problem is to compensate the sensor dynamics and enlarge working ranges of each sensor as shown in Fig.1(a). Based on this, Baerveldt and Klang [12] and Hadri and Benallegue [13] succeeded to improve the accuracy of estimation. The former dealt only with rotation about one axis, and the latter considered no interference. In the case of 3D rotation, the sensor dynamics displays a highly nonlinear property. Even if it is approximated by a linear system, the inverse models of sensors tend to be non-proper and unstable.

We propose a novel technique to overcome the above problem, where the inverse model of sensors are decoupled into the dynamics compensation part and the coordinate transformation part as shown in Fig.1(b). The former part is approximated by a linear transfer function, while the latter part is computed in strict nonlinear form. Then, bandpass filters are designed and inserted *before* the coordinate transformation in order to guarantee that the total transfer function becomes proper and stable. Particularly, the differential operator of a high-pass filter cancels the integral operator included in the dynamics compensation of the rate gyroscope, which causes instability. Experimental results show that the proposed method substantially improves the fidelity of the estimation even in fast and irregular movements up to 5[Hz].

II. Complementary filter with decoupled linear and nonlinear properties

The complementary filter [5], as its name explains, combines signals from heterogeneous sensors in a complementary manner in order to improve the accuracy of estimation. It is designed in the frequency domain where each sensor signal in the reliable frequency range is filtered and synthesized. The following equation represents the basic idea of linear complementary filter:

$$\boldsymbol{Y}(s) = \sum_{i=1}^{n} \boldsymbol{F}_i(s)\boldsymbol{X}_i(s), \tag{1}$$

where $\boldsymbol{Y}(s)$ is the estimated value, $\boldsymbol{X}_i(s)$ is the ith sensor output and $\boldsymbol{F}_i(s)$ is the bandpass filter for the ith sensor. For the attitude estimation, for example, $\boldsymbol{F}_i(s)$ is defined as a low-pass filter for an inclinometer, while it is defined as a high-pass filter for a rate gyroscope. As long as the

This work was supported in part by Grant-in-Aid for Young Scientists (A) #22680018, Japan Society for the Promotion of Science and by "The Kyushu University Research Superstar Program (SSP)", based on the budget of Kyushu University allocated under President's initiative.

K. Masuya is with the Department of Mechanical Engineering, Kyushu University. E-mail:masuya@ctrl.mech.kyushu-u.ac.jp.

T. Sugihara is with the Department of Adaptive Machine Systems, Osaka University. E-mail: zhidao@ieee.org.

M. Yamammoto is with the Department of Mechanical Engineering, Kyushu University. E-mail: yama@mech.kyushu-u.ac.jp

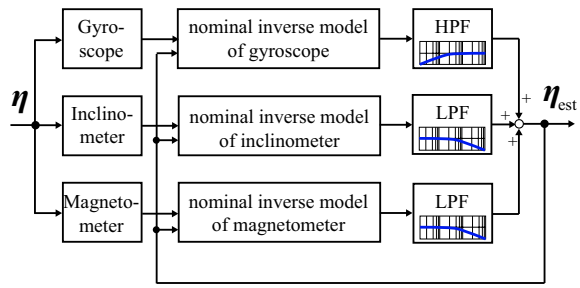

(a) the original idea with a compensation of sensor dynamics

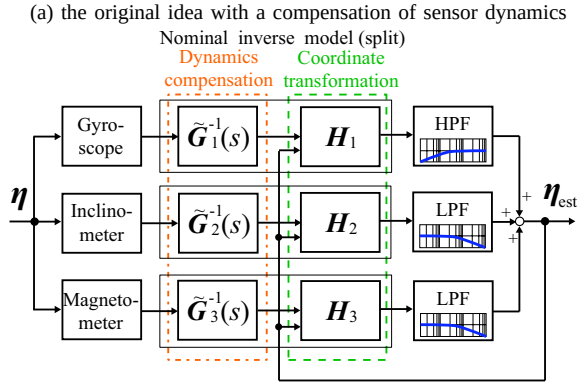

(b) a revised idea with a sensor dynamics which is splitted into a linear transfer function and the coordinate transformation

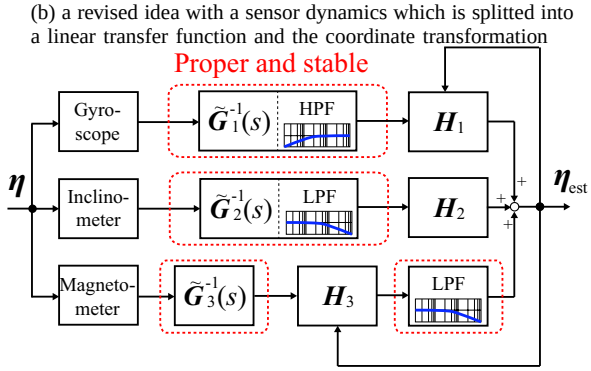

(c) the proposed idea to guarantee the properness and stability where a bandpass filter is inserted between the linear transfer function and the coordinate transformation

Fig. 1. Complementary filter for attitude estimation

following condition is satisfied, the filter designed based on Eq.(1) consistently estimates the original signal.

$$\sum_{i=1}^{n} \boldsymbol{F}_i(s) = \mathbf{1}, \tag{2}$$

where $\mathbf{1}$ is unit matrix.

The problem lies in a fact that the reliable frequency domains of each sensor are not necessarily complementary. Due to that, the accuracy of estimation is degraded in the frequency range without any reliable sensor signals. In the case of a combination of an inclinometer and a rate gyroscope, the former is easily affected by translational movements and its working range is low. An idea against this concern is to insert inverse models of each sensor before the bandpass filters in order to compensate the sensor dynamics which causes substantial delays of the outputs as Fig.1(a) depicts. In the case of 3D rotation, however, the sensor dynamics displays a highly nonlinear property. Even if it is approximated by a linear system, the inverse models of the sensors often become non-proper or unstable. Particularly, the inverse model of the rate gyroscope includes a rather complex spherical integration operator which accumulates the drift of the output and that operator makes the system unstable in linear approximation.

In order to overcome the above problem, we propose a novel technique. First, the inverse model of a sensor is decoupled into the sensor dynamics compensation part and the coordinate transformation part as in Fig.1(b). The former part is approximated by a linear transfer function, while the latter part is based on the strict nonlinear computation. This computation is represented by the following equation:

$$\boldsymbol{\eta}_{\mathrm{est}} = \sum_{i=1}^{n} \boldsymbol{F}_i(s)\boldsymbol{H}_i\left(\tilde{\boldsymbol{G}}_i^{-1}(s)\boldsymbol{X}_i(s)\right), \tag{3}$$

where $\boldsymbol{\eta}_{est}$ is the estimation of the original attitude $\boldsymbol{\eta}$, $\boldsymbol{H}_i(\cdot)$ is the coordinate transformation from the ith sensor frame to the inertial frame, and $\tilde{\boldsymbol{G}}_i(s)$ is a nominal linearized dynamics model of the ith sensor.

Then, the bandpass filters are inserted between those split parts. Since the bandpass filters are also designed as linear transfer function, they are merged with the dynamics compensation part as depicted in Fig.1(c). The merged system can be made proper and stable by carefully designing each filter. This means that Eq.(3) is modified as follows:

$$\boldsymbol{\eta}_{\mathrm{est}} = \sum_{i=1}^{n} \boldsymbol{H}_i\left(\boldsymbol{F}_i(s)\tilde{\boldsymbol{G}}_i^{-1}(s)\boldsymbol{X}_i(s)\right), \tag{4}$$

where the system $\boldsymbol{F}_i(s)\tilde{\boldsymbol{G}}_i^{-1}(s)$ for any sensor is proper and stable. The reason why such swapping of the order of process is acceptable depends on the types of sensors. The detail is described in the following section.

III. Implementation of the Complementary Filter

A. Representation of 3D attitude

In this paper, attitude is defined by angles shown in Fig.2 and is parameterized by $\boldsymbol{\eta} = [\theta_1\ \theta_2\ \phi]^{\mathrm{T}}$ where θ_1 and θ_2 represent the inclination and ϕ represents the azimuth. By that representation, the attitude matrix of the sensor frame with respect to the inertial frame is obtained as follows,

$$\boldsymbol{R} = \boldsymbol{R}_\phi \boldsymbol{R}_\theta, \tag{5}$$

where $\boldsymbol{R}_\theta$ is

$$\boldsymbol{R}_\theta = \begin{bmatrix} \kappa/\cos\theta_1 & \kappa\sin\theta_1\tan\theta_2 & \kappa\tan\theta_2\cos\theta_1 \\ 0 & \cos\theta_1 & -\sin\theta_1 \\ -\kappa\tan\theta_2 & \kappa\tan\theta_1 & \kappa \end{bmatrix}, \tag{6}$$

$$\kappa \equiv \frac{1}{\sqrt{1+\tan^2\theta_1+\tan^2\theta_2}}, \tag{7}$$

and $\boldsymbol{R}_\phi$ is

$$\boldsymbol{R}_\phi = \begin{bmatrix} \cos\phi & -\sin\phi & 0 \\ \sin\phi & \cos\phi & 0 \\ 0 & 0 & 1 \end{bmatrix}. \tag{8}$$

Therefore, by Eqs.(5), (6) and (8), $\boldsymbol{R}$ is

$$\boldsymbol{R} = \begin{bmatrix} \kappa C_\phi/C_1 & -C_1S_\phi+\kappa C_\phi S_1T_2 & S_\phi S_1+\kappa C_\phi C_1T_2 \\ \kappa S_\phi/C_1 & C_\phi C_1+\kappa S_\phi S_1T_2 & -C_\phi S_1+\kappa C_1S_\phi T_2 \\ -\kappa T_2 & \kappa T_1 & \kappa \end{bmatrix}, \tag{9}$$

where the subscripts $1, 2$and ϕ mean θ_1, θ_2 and ϕ respectively and C_i, S_i and T_i $(i = 1, 2, \phi)$ mean cosine, sine and tangent respectively.

B. The coordinate transformation

For the gyroscope, the integrated value of the angular velocity vector $\boldsymbol{\omega}$ is transformed to $\boldsymbol{\eta}$ by nonlinear function originally. However, the integration has no physical meaning, so that following sequence is considered. First, the angular velocity vector $\boldsymbol{\omega}$ is transformed to the rates of attitude $\dot{\boldsymbol{\eta}}$. After that, $\dot{\boldsymbol{\eta}}$ is integrated and filtered by high-pass filter. Therefore, we define the transformation from $\boldsymbol{\omega}$ to $\dot{\boldsymbol{\eta}}$ as the coordinate transformation. By the swap of the order of the coordinate transformation and filtering process in later subsection, the differential operator included in high-pass filter cancels the integral operator. As a result, it is equal to the sequence which is transformation after the sensor output is integrated and filtered.

The rate gyroscope outputs the angular velocity ${}^b\boldsymbol{\omega}$ of the sensor frame where its direction is with respect to the sensor frame itself. Namely,

$$\boldsymbol{\omega} = \boldsymbol{R}\,{}^b\boldsymbol{\omega} \Leftrightarrow {}^b\boldsymbol{\omega} = \boldsymbol{R}^{\mathrm{T}}\boldsymbol{\omega}. \tag{10}$$

By using Rodrigue's formula, the variation of attitude matrix in micro time is obtained as follows:

$$\mathrm{d}\boldsymbol{R} = \boldsymbol{1} - \frac{\boldsymbol{\omega}_\times}{\|\boldsymbol{\omega}\|}\sin(\|\boldsymbol{\omega}\|\mathrm{d}t) + \frac{(\boldsymbol{\omega}_\times)^2}{\|\boldsymbol{\omega}\|^2}\left(1 - \cos(\|\boldsymbol{\omega}\|\mathrm{d}t)\right), \tag{11}$$

where $\boldsymbol{\omega}_\times$ is the matrix which represents the cross product with $\boldsymbol{\omega}$. In practice, the latest estimation of $\boldsymbol{R}$ in the previous step is available instead of the current attitude. From Eq.(9), the variation $\mathrm{d}\boldsymbol{\eta}$ in $\mathrm{d}t$ is

$$\mathrm{d}\boldsymbol{\eta} = \begin{bmatrix} \mathrm{atan2}(\mathrm{d}r_{32}, \mathrm{d}r_{33}) \\ -\mathrm{atan2}(\mathrm{d}r_{31}, \mathrm{d}r_{33}) \\ \mathrm{atan2}(\mathrm{d}r_{21}, \mathrm{d}r_{22}) \end{bmatrix}, \tag{12}$$

where $\mathrm{d}r_{ij}$ represents the ith row and jth column element of $\mathrm{d}\boldsymbol{R}$. When implementing this in a discretized form, $\mathrm{d}t$ is approximated by sampling time ΔT, we define the coordinate transformation $\boldsymbol{H}_1({}^b\boldsymbol{\omega})$ which do ${}^b\boldsymbol{\omega}$ to $\dot{\boldsymbol{\eta}}$ as follows:

$$\boldsymbol{H}_1({}^b\boldsymbol{\omega}) \equiv \frac{\mathrm{d}\boldsymbol{\eta}}{\mathrm{d}t} \simeq \frac{\Delta\boldsymbol{\eta}}{\Delta t}. \tag{13}$$

Also, the output of the inclinometer ξ_1 and ξ_2 correspond to the inclination θ_1 and θ_2 respectively. That of the magnetometer $\boldsymbol{m} \in \mathbb{R}^3$ is affected by not only the azimuth but the inclination. The azimuth ϕ is that the vector $\boldsymbol{R}_\theta^{\mathrm{T}}\boldsymbol{m} = [x_m\ y_m\ z_m]^{\mathrm{T}}$ which is compensated by $\boldsymbol{R}_\theta$ makes with the initial vector $\boldsymbol{m}_0 = [x_{m0}\ y_{m0}\ z_{m0}]^{\mathrm{T}}$. Therefore, we define the coordinate transformation of inclinometer $\boldsymbol{H}_2(\xi_1, \xi_2)$ and that of magnetometer $\boldsymbol{H}_3(\boldsymbol{m})$ as follows:

$$\boldsymbol{H}_2(\xi_1, \xi_2) \equiv [\xi_1 \quad \xi_2 \quad 0]^{\mathrm{T}}, \tag{14}$$

$$\boldsymbol{H}_3(\boldsymbol{m}) \equiv \begin{bmatrix} 0 \\ 0 \\ \mathrm{atan2}(x_m y_{m0} - y_m x_{m0}, x_m x_{m0} + y_m y_{m0}) \end{bmatrix}, \tag{15}$$

where the angle, which we don't get, is regarded as zero. These values obtained by both transformations are treated as the estimation in low frequency range.

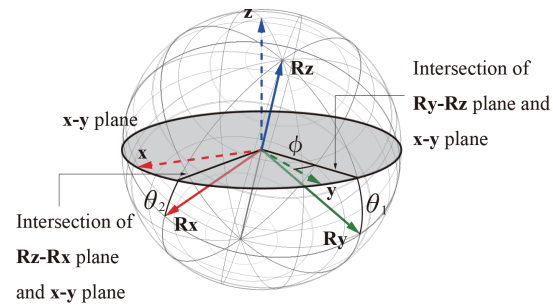

Fig. 2. The inclination and azimuth

C. Linear approximation of sensor dynamics

Although the actual sensor dynamics is non-linear due to the interference of movements along various directions, we assume that it is approximated by a linear transfer function and the interference between movements about independent axes are linearly separable. A support for this assumption is that the commercial sensors are designed so as to reduce the effect of movements other than that in the direction of interest. Based on the above, the nominal dynamics of the rate gyroscope $\tilde{\boldsymbol{G}}_1(s)$, the inclinometer $\tilde{\boldsymbol{G}}_2(s)$ and the magnetometer $\tilde{\boldsymbol{G}}_3(s)$ are represented as follows:

$$\tilde{\boldsymbol{G}}_1(s) = s\begin{bmatrix} \frac{K_{11}}{D_1(s)} & \frac{K_{12}}{D_1(s)} & \frac{K_{13}}{D_1(s)} \\ \frac{K_{21}}{D_2(s)} & \frac{K_{22}}{D_2(s)} & \frac{K_{23}}{D_2(s)} \\ \frac{K_{31}}{D_3(s)} & \frac{K_{32}}{D_3(s)} & \frac{K_{33}}{D_3(s)} \end{bmatrix}, \tag{16}$$

$$\tilde{\boldsymbol{G}}_2(s) = \frac{1}{D(s)}\begin{bmatrix} 1 & k_1 \\ k_2 & 1 \end{bmatrix}, \tag{17}$$

$$\tilde{\boldsymbol{G}}_3(s) = \begin{bmatrix} M_{11} & M_{12} & M_{13} \\ M_{21} & M_{22} & M_{23} \\ M_{31} & M_{32} & M_{33} \end{bmatrix}. \tag{18}$$

We empirically verified that the denominators of $\tilde{\boldsymbol{G}}_1(s)$ are all by linear functions, $D(s)$ is well-approximated by a quadratic function and $\tilde{\boldsymbol{G}}_3(s)$ are all constant. They can be identified by examining the frequency responses between one of the components of the input and one of the components of the output of each sensor and applying the least square method. An example process will be shown in the next section. Based on them, the inverse model of sensor dynamics are obtained as $\tilde{\boldsymbol{G}}_1^{-1}(s)$, $\tilde{\boldsymbol{G}}_2^{-1}(s)$ and $\tilde{\boldsymbol{G}}_3^{-1}(s)$.

Note that $\tilde{\boldsymbol{G}}_1^{-1}(s)$ includes the integration operator 1/s. We know that it is mathematically incorrect to apply the integration to the angular velocity. However, it is totally cancelled by the high-pass filter, so that it doesn't harm the approximation.

D. the swap of the order of the coordinate transformation and filtering process

It should be explained why the swap of the order of the coordinate transformation and filtering process is accepted. Concerning with the inclinometer, from the coordinate transformation defined by Eq.(14), the swap is trivial. Also, $\tilde{\boldsymbol{G}}_3^{-1}(s)$ is constant matrix, so that the swap isn't necessary.

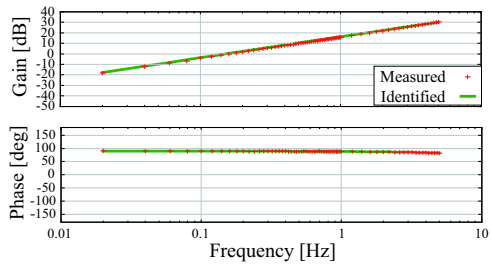

(a) Example of frequency response around primary axis ($\tilde{\boldsymbol{G}}_{1,11}$).

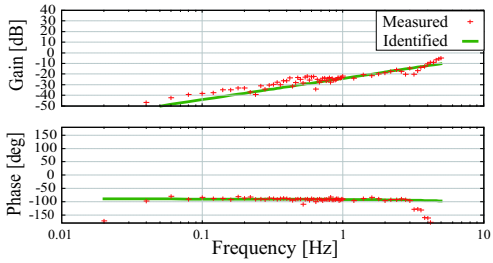

(b) Example of frequaency response around interfering axis ($\tilde{\boldsymbol{G}}_{1,23}$).

Fig. 3. Bode diagram of rate gyroscope

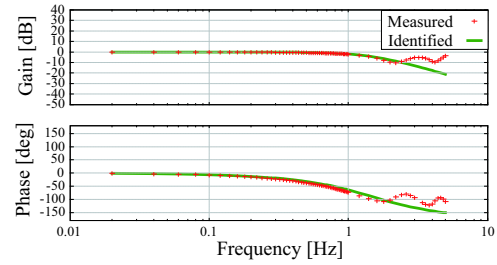

(a) Example of frequency response around primary axis ($\tilde{\boldsymbol{G}}_{2,11}$).

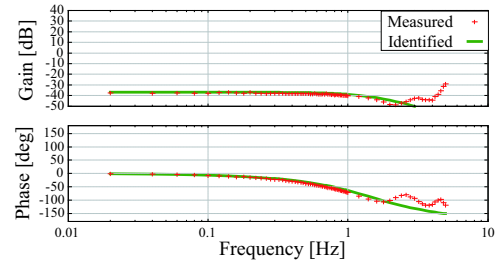

(b) Example of frequaency response around interfering axis ($\tilde{\boldsymbol{G}}_{2,12}$).

Fig. 4. Bode diagram of inclinometer

The reason is not very clear in the case of the gyroscope. Given that $\|\boldsymbol{\omega}\|\Delta T \ll 1$, Eq.(11) is approximated as follows:

$$\mathrm{d}\boldsymbol{R} \simeq \boldsymbol{I} - \frac{\boldsymbol{\omega}_\times}{\|\boldsymbol{\omega}\|}\|\boldsymbol{\omega}\|\Delta T = \boldsymbol{I} - \boldsymbol{\omega}_\times \Delta T. \tag{19}$$

Then, Eq.(12) is rewritten by Taylor expansion,

$$\boldsymbol{H}_1({}^b\boldsymbol{\omega}) \quad \simeq \quad \boldsymbol{R}\,{}^b\boldsymbol{\omega} + (1/\Delta T)O\left((\boldsymbol{R}\,{}^b\boldsymbol{\omega}\Delta T)^3\right), \tag{20}$$

where $O(\boldsymbol{v}^3)$ represents 3D vector $[O(v_x^3) \;\; O(v_y^3) \;\; O(v_z^3)]^{\mathrm{T}}$ for the vector $\boldsymbol{v} = [v_x \;\; v_y \;\; v_z]^{\mathrm{T}}$. Hence,

$$\boldsymbol{H}_1(\boldsymbol{F}\,{}^b\boldsymbol{\omega}) \simeq \boldsymbol{R}\boldsymbol{F}\,{}^b\boldsymbol{\omega} + (1/\Delta T)O\left((\boldsymbol{R}\boldsymbol{F}\,{}^b\boldsymbol{\omega}\Delta T)^3\right), \tag{21}$$

$$\boldsymbol{F}\boldsymbol{H}_1({}^b\boldsymbol{\omega}) \simeq \boldsymbol{F}\boldsymbol{R}\,{}^b\boldsymbol{\omega} + \boldsymbol{F}(1/\Delta T)O\left((\boldsymbol{R}\,{}^b\boldsymbol{\omega}\Delta T)^3\right). \tag{22}$$

If $\boldsymbol{F}_1(s) = F_1(s)\mathbf{1}$, then we get $\boldsymbol{F}\boldsymbol{R} \simeq \boldsymbol{R}\boldsymbol{F}$. Now, we know they coincide with each other up to the second order term, so that one may say the former well approximates the latter and it causes no serious problem.

IV. Experiments

A. Sensors and identification of dynamics

This section presents an example of the implementation of the proposed method. We adopted X3M (US Digital) as the inclinometer, CRS07-11S (Silicon Sensing Systems Japan) as the rate gyroscope and AMI304(Aichi Micro Intelligent) as the magnetometer. X3M internally measures the acceleration due to the gravity and AMI304 measures terrestrial magnetism. These outputs digital signal so that it less suffers from analog noises. CRS07-11S is a small vibrating structure gyro with less drifts. They are not very expensive (several hundreds of US dollars) and easily available. In spite of small signal noises and drifts on them, they are individually still imperfect as well as other inertial sensors.

First, the transfer functions of each sensor are identified. The experimental table rotates about three orthogonal axes independently. Each axis is controlled by a servo system with a high-gain PID compensator.

By applying a sinusoidal reference to the servo controller, a response of the table and the sensor is measured in cases of the gyroscope and the inclinometer. We collected 3 responses for each frequency from 0.02[Hz] to 5[Hz]. Then, gain and phase lag from the table to the sensor for each frequency are identified through the least square method and plotted on a bode diagram. Figs.3 and 4 are examples of the resulted Bode diagrams. The transfer function is also identified through the least square method as

$$\tilde{\boldsymbol{G}}_1(s) = s\begin{bmatrix} \frac{1.035686}{1+0.004112s} & \frac{-0.025885}{1+0.004112s} & \frac{0.005136}{1+0.004112s} \\ \frac{0.034362}{1+0.004177s} & \frac{1.070075}{1+0.004177s} & \frac{-0.009853}{1+0.004177s} \\ \frac{-0.038275}{1+0.004858s} & \frac{0.029495}{1+0.004858s} & \frac{1.075213}{1+0.004858s} \end{bmatrix}, \tag{23}$$

$$\tilde{\boldsymbol{G}}_2(s) = \frac{1}{D(s)}\begin{bmatrix} 1 & 0.01431 \\ 0.01904 & 1 \end{bmatrix}, \tag{24}$$

where

$$D(s) = 1 + 0.1788s + 0.0113609s^2 \tag{25}$$

and the order of each function is empirically determined. Note that $\tilde{\boldsymbol{G}}_1^{-1}(s)$ is unstable and $\tilde{\boldsymbol{G}}_2^{-1}(s)$ is non-proper.

In case of the magnetometer, the terrestrial magnetism, which is varied sinusoidally by rotating table around vertical axis at constant angular velocity Ω, is input to the sensor. Then, gain and phase are identified through the least square method and normalized as that x direction's gain is equal to 1. Figs.5 shows the resulted Bode diagram. The transfer function is assumed as the diagonal matrix, so that the

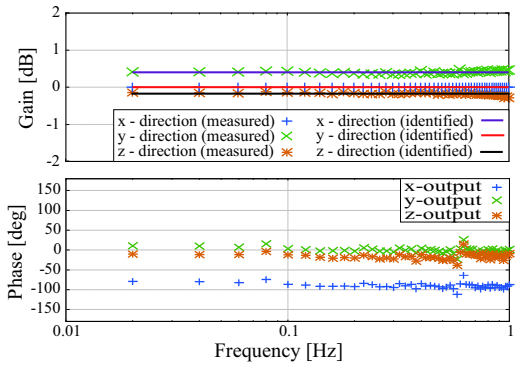

Fig. 5. Bode diagram of magnetometer

function is

$$\tilde{\boldsymbol{G}}_3(s) = \mathrm{diag}\{1.0,\ 1.048,\ 0.980\}. \tag{26}$$

B. Design of complementary bandpass filter

The Bode diagrams also tell the reliable frequency range of each sensor. In our case, the dynamics of X3M is well approximated by the identified function up to about 1[Hz], while that of CRS07-11S rather shows a good property in a wide range. In order to make $\boldsymbol{F}_2(s)\tilde{\boldsymbol{G}}_2^{-1}(s)$ proper, $\boldsymbol{F}_2(s)$ must be the second or more order lag system. Then, we define the complementary filters as

$$\boldsymbol{F}_1(s) = \frac{(1/3)s(1+(1/12)s)}{(1+(1/6)s)^2}\mathbf{1}, \tag{27}$$

$$\boldsymbol{F}_2(s) = \frac{1}{(1+(1/6)s)^2}\mathrm{diag}\{1,\ 1,\ 0\}, \tag{28}$$

$$\boldsymbol{F}_3(s) = \frac{1}{(1+(1/6)s)^2}\mathrm{diag}\{0,\ 0,\ 1\}, \tag{29}$$

where $\boldsymbol{F}_1$ has high-pass characteristics and $\boldsymbol{F}_2$ and $\boldsymbol{F}_3$ have low-pass characteristics, and they satisfy complementary condition. Moreover, since $\boldsymbol{F}_1(s)$ has the differential operator s, which cancels the integral operator of $\tilde{\boldsymbol{G}}_1^{-1}(s)$ and makes $\boldsymbol{F}_1(s)\tilde{\boldsymbol{G}}_1^{-1}(s)$ stable. It also resolves mathematically incorrect integration of the angular velocity.

C. Results

The performance of the designed complementary filter was examined on the same testing table. The rotating motion to be estimated was composed of the following functions:

$$q_i(t) = \sum_{j=1}^{5}\left(a_{ij}\sin(2\pi f_{ij}t) + b_{ij}\cos(2\pi f_{ij}t)\right), \tag{30}$$

where the coefficients a_{ij} and b_{ij} and the frequency f_{ij} up to 5[Hz] were chosen at random as shown in Table I. The sampling time was 3[ms] and the total time was 30[s].

Fig.6 shows the results of estimations by the proposed method and the conventional methods from 0[s] to 10[s]. For comparison, Yun et al.'s method[3] was also examined as a representative of nonlinear Kalman filters. The errors between the estimated and true values including that of Kalman filter without tuning are plotted in Fig.7. Root-mean-square error and standard deviation of those results are shown in Table II. One can notice that RMSE of inclination significantly decreases by about 80% and that of azimuth also does by about 50% compared with the filter without inverse model. The result shows that the estimation is affected by sensor dynamics. Therefore, the proposed method has a better performance over the method without sensor dynamics compensation. On the other hand, RMSE of inclination significantly decreases by 60% compared with Kalman filter without tuning and there aren't much difference in RMSE of proposed filter and Kalman filter with tuning. These results shows that Kakman filter estimates as accurate as the proposed filter by tuning. However, tuning of Kalman filter by trial and error takes more time than the proposed filter to estimate accurately. In fact, we repeated it about 80 times to get this result. Therefore, in terms of the implementation, the proposed method has more advantage.

TABLE I

THE INPUT PARAMETER

j	a_{1j}	b_{1j}	f_{1j}	a_{2j}	b_{2j}	f_{2j}	a_{3j}	b_{3j}	f_{3j}
1	7.99	1.40	0.48	7.62	4.37	0.53	6.96	2.12	0.82
2	7.29	6.50	1.07	0.99	0.28	1.64	4.54	6.20	1.92
3	5.79	4.74	2.19	6.91	5.36	2.21	8.47	7.41	2.26
4	2.90	7.20	3.31	1.69	11.1	3.68	9.23	11.2	3.02
5	6.50	2.28	4.03	10.2	0.28	4.00	3.03	7.41	4.03

TABLE II

THE ESTIMATE ERROR

	Angle	RMSE	SD	Mean
Proposed filter	$\theta_{1,\mathrm{est}}$	2.18	2.18	0.04
	$\theta_{2,\mathrm{est}}$	2.01	1.89	-0.70
	ϕ_{est}	2.65	2.64	-0.24
Filter without inverse model	$\theta_{1,\mathrm{est}}$	11.1	11.1	0.40
	$\theta_{2,\mathrm{est}}$	8.91	8.90	-0.36
	ϕ_{est}	5.40	5.33	-0.84
Yun et al.'s KF (without tuning)	$\theta_{1,\mathrm{est}}$	5.17	5.16	-0.29
	$\theta_{2,\mathrm{est}}$	3.89	3.85	0.62
	ϕ_{est}	2.52	2.15	1.32
Yun et al.'s KF (with tuning)	$\theta_{1,\mathrm{est}}$	2.00	1.99	-0.22
	$\theta_{2,\mathrm{est}}$	2.40	2.16	-1.06
	ϕ_{est}	2.44	2.05	-1.33

RMSE $\cdots$ root-mean-square error
SD $\cdots$ Standard Deviation

V. CONCLUSIONS

In this research, we proposed a novel technique to improve the accuracy of the attitude estimation by heterogeneous inertial sensors. By using inverse model of each sensor, we designed the complementary filter which enlarge each reliable frequency range. The inverse model is decoupled into the linear dynamics compensation part and the nonlinear coordinate transformation part. Then, bandpass filters are inserted before the coordinate transformation in order to guarantee that the total transfer function becomes proper and stable. The experimental results shows that the proposed filter is more accurate than the filter without inverse model and Kalman filter without tuning. The proposed method is more beneficial than Kalman filter in terms of the implementation since it facilitates a systematic design of the filter.

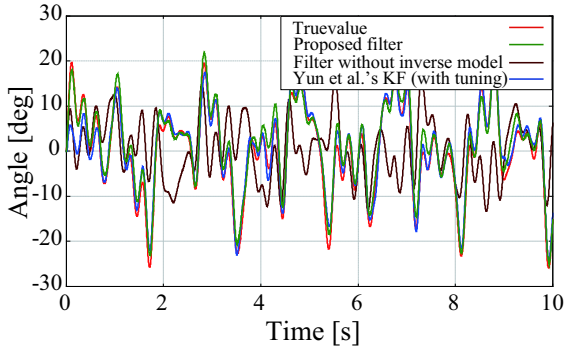

(a) The estimate $\theta_{1,est}$

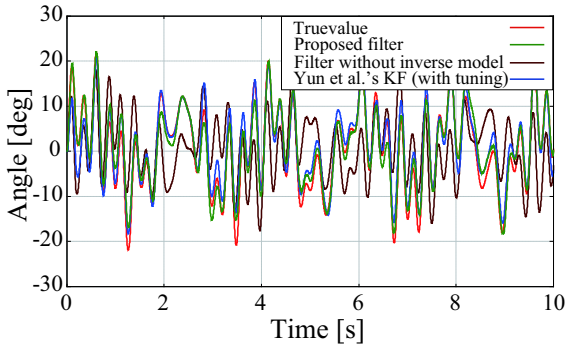

(b) The estimate $\theta_{2,est}$

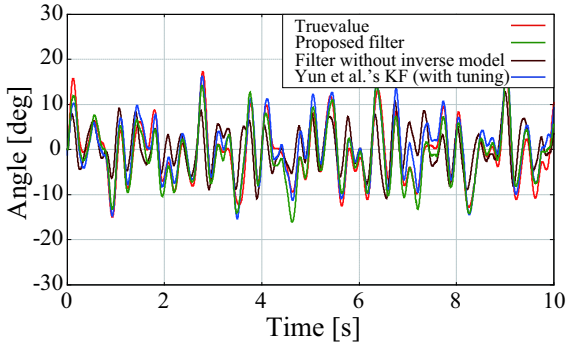

(c) The estimate ϕ_{est}

Fig. 6. The estimation result of proposed filter and Kalman filter

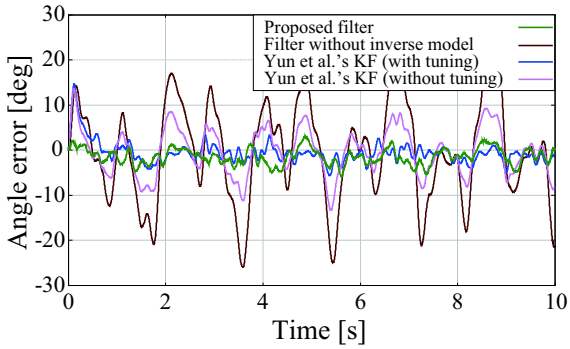

(a) The error of $\theta_{1,est}$

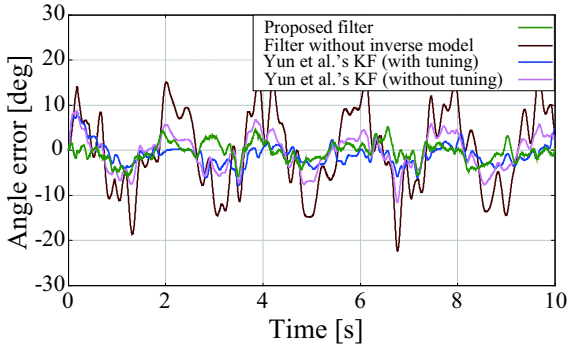

(b) The error of $\theta_{2,est}$

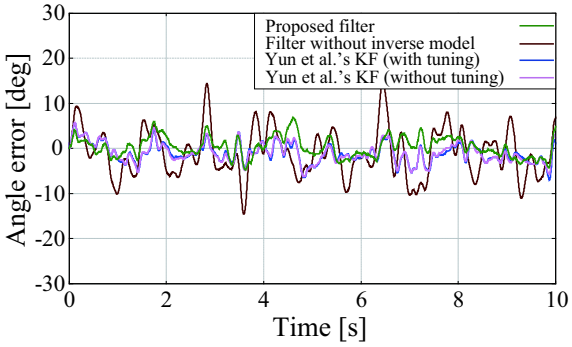

(c) The error of ϕ_{est}

Fig. 7. The error result of proposed filter and Kalman filter

REFERENCES

[1] E. J. Lefferts, F. L. Markley, and M. D. Shuster, *Kalman Filtering for Spacecraft Attitude Estimation*, Journal of Guidance, Control and Dynamics, vol.5, No.5, pp.417-429, 1982.

[2] G. Creamer, *Spacecraft Attitude Determination Using Gyros and Quaternion Measurements*, The Journal of the Astronautical Sciences, vol.44, No.3, pp.357-371, 1996.

[3] X. Yun, C. Aparicio, E. R. Bachmann and R. B. McGhee, *Implementation and Experimental Results of a Quaternion-Based Kalman Filter for Human Body Motion Tracking*, Proceedings of the 2005 IEEE International Conference on Robotics and Automation, pp.317-322, 2005.

[4] S. Suzuki, M. Tawara, D. Nakazawa, and K. Nonami, *Research on Attitude Estimation Algorithm under Dynamic Acceleration (in Japanese)*, Journal of the Robotics Society of Japan, Vol.26, No.6, pp.626-634, 2008

[5] W. H. Wrikler, *Aircraft Course Stabilizing Means*, U. S. Patent 2,548,278, 1951-04-10.

[6] R. Mahony, T. Hamel, and J. M. Pflimlin, *Complementary filter design on the special orthogonal group*, In Proceeding of the 44th IEEE Conference on Decision and Control, and the European Control Conference 2005, pp.1477-1484, 2005.

[7] R. Mahony, T. Hamel, and J. M. Pflimlin, *Nonlinear Complementary filter on the Special Orthogonal Group*, IEEE Transactions on Automatic Control, vol.53, No.5, pp.1203-1218, 2008.

[8] Y. Li, *A Filter Design Method for Robot Tip Velocity Derivation*, JSME international journal. Series C, Vol.40, No.1, pp.82-88, 1997.

[9] M. Euston, P.Coote, R.Mahony, J. Kim, and T. Hamel, *A Complementary Filter for Attitude Estimation of a Fixed-Wing UAV*, in the Proceedings of 2008 IEEE/RSJ International Conference of Intelligent Robots and Systems, pp.340-345, 2008.

[10] J. F. Vasconcelos, C. Silvestre, P. Oliveira, P. Batista, and B. Cardeira, *Discrete Time-Varying Attitude Complementary Filter*, American Control Conference 2009, pp.4056-4061, 2009

[11] J. M. Roberts, P. I. Corke, and G. Buskey, *Low-Cost Flight Control Systems for a Small Autonomous Helicopter*, in the Proceedings of Australasian Conference on Robotics and Automation, pp.71-76, 2002.

[12] A. J. Baerveldt, and R. Klang, *A Low-cost and Low-weight Attitude Estimation System for an Autonomous Helicopter*, Intelligent Engineer Systems, pp.391-395, 1997

[13] A. El Hadri, and A. Benallegue, *Attitude estimation with gyros-bias compensation using low-cost sensors*, Proceeding of the 48th Conference on Decision and Control, pp.8077-8082, 2009.